



NOVA

University of Newcastle Research Online

nova.newcastle.edu.au

Bhatia, Shashank; Chalup, Stephan K.; Ostwald, Michael J. "Wayfinding: a method for the empirical evaluation of structural saliency using 3D Isovists", *Architectural Science Review* Vol. 56, Issue 3, p. 220-231 (2013)

Available from: <http://hdl.handle.net/1959.13/1047666>

This is an electronic version of an article published in *Architectural Science Review*, 56:3, 220-231 (2013).

*Architectural Science Review* is available online at:

<http://www.tandfonline.com/doi/abs/10.1080/00038628.2013.811635>

**Accessed from:** <http://hdl.handle.net/1959.13/1047666>

## **Wayfinding: A method for the empirical evaluation of structural saliency using 3D Isovists**

Shashank Bhatia, Stephan K. Chalup, Michael J. Ostwald

*Faculty of Engineering and Built Environment, University of Newcastle, Callaghan, Australia.*

[Shashank.bhatia@uon.edu.au](mailto:Shashank.bhatia@uon.edu.au)

Room ES-107

Faculty of Engineering and Built Environment

The University of Newcastle

University Drive

Callaghan – 2308.

Australia

Shashank Bhatia is a post-graduate research student at the School of Electrical Engineering and Computer Science, The University of Newcastle.

# **Wayfinding: A method for the empirical evaluation of structural saliency using 3D Isovists**

The presence of locations that possess distinct spatial-cognitive features (salient landmarks) is a fundamental necessity for supporting navigation. Embedding formal or structural variability sufficient to create such landmark locations is therefore an important consideration in the design of large urban and architectural spaces. Despite the availability of diverse theories that seek to identify the characteristics of “a salient landmark”, relatively few experimental techniques are available to empirically evaluate saliency in a given architecture plan. This study is therefore motivated by the development of an ability to measure spatial distinctiveness during the architectural design and modelling process. The information from such an analysis can prove useful for evaluating the way in which a design provides support for wayfinding and spatial appeal. Statistical summaries obtained from the 3D isovists are compared using principal component analysis to differentiate monotonous regions from the more structurally distinct ones. The experiments reported in the paper demonstrate novel utilisation of the isovist concept to capture spatial properties and comparison of structural saliency amongst two well-known architectural designs. Central contributions of the paper include the novel experimentation technique of capturing and utilising 3D isovists, its interpretation and the quantitative methodology behind saliency computation.

Keywords: 3D isovists; structural saliency; computational analysis; design analysis; spatial cognition; dimensionality reduction

Subject classification codes: design analysis

## **1. Introduction**

One of the questions that spatial psychologists and architectural designers repeatedly ask is, “why do people get lost in buildings” (Carlson *et al.* 2010; 284)? While many factors influence the answer to this question, it has been demonstrated that

the quantity and quality of visual information that is available to a person, from a given location in space, is critical to the generation of coherent mental maps (Golledge 1999; Conroy-Dalton 2005). Moreover, this information is always relative, both within the immediate experience of a building or space, and in relation to the larger set of buildings or spaces that a person has experienced in their lives. Thus, a central property of spatial cognition is a capacity for identifying or expressing difference. This is why buildings and cities that possess relatively uniform or undifferentiated spatial properties are typically regarded as being both lacking in identity and being difficult to navigate around (Lynch 1960; Ellard 2009). Significantly, Carlson (*et al.* 2010) describes such spaces as promoting loss of orientation because they lack “salient landmarks” (287). However, locations with differing levels of spatial information, and especially those that possess a high level of contrasting geometric information have a propensity to be remembered as critical orientation sites (Conroy-Dalton 2001; Haq and Giroto 2003). Montello (1998) elaborates that such sites “serve important roles in the organization of spatial knowledge” (144), even though, they “do not in themselves contain spatial information” (144) that is useful; it is only through comparison with other information in the system that they became significant. Viewed in this way, questions about wayfinding and spatial identity in architecture could be regarded as relating directly to the presence, or absence, of salient features.

Since the 1970s, architects, planners and urban designers have attempted to develop methods for the analysis of the visual properties of space that relate to mental maps and wayfinding (Meilinger *et al.* 2009). Many of these have relied on studies of human experience to produce results (Baskaya *et al.* 2004, Werner 2004, Wiener and Franz 2005, Wiener *et al.* 2007). Interest in the geometric properties of vision, often formalized into a study of isovists properties (Benedikt 1979; Turner *et al.* 2001) also

posed great potential for this field of research, but have not since been developed specifically to study issues of visual saliency. This is not surprising given that the accurate modeling and estimation of the degree of geometric visual character – what might be called structural salience – is a challenging task. Several factors including isovist visibility, geometric shape, extent of visual area and the shape enclosed around the vantage point all need to be evaluated. Furthermore, accounting for these factors and comparing them over many hundreds of vantage locations can prove to be physically impossible and computationally intensive. Recent contributions in this field propose experimental methods employing human subjects to evaluate different vantage locations in virtual environments and provide subjective feedback (Caduff, & Timpf 2008; Duckham, et al. 2010; Han, et al. 2012; Hirtle 2008; Hochdorfer and Schlegel 2009; Miller and Carlson 2010; Peters et al. 2010; Röser et al. 2012a; Röser et al. 2012b; Winter et al. 2008). The nature of feedback varies from spatial descriptions (Miller & Carlson 2010), to choice of landmarks (Peters et al. 2010) and route descriptions (Röser et al. 2012). This paper approaches this complex issue by demonstrating a repeatable method for evaluating the wayfind-ability of complex architectural and urban environments. Specifically, the paper proposes a computational methodology employing 3D isovists for determining structural salience. The application of 3D isovists is intended to imitate, as closely as possible, human visual perception. This property, in comparison to alternative social sciences approaches, has a potential universal application. It also ensures that the resolution of saliency is reliant on what is directly visible, rather than what could be inferred indirectly. It derives its theory and application from architectural science and computing and it depends on concepts derived from the field of computer science to evaluate overall features responsible for structural saliency.

The experiments reported in the present paper demonstrate the application of a new saliency estimation method using hypothetical architectural models and two canonical house designs; the *Villa Savoye* at Poissy (near Paris, France) by Le Corbusier, and the *Dana-Thomas House* at Springfield (Illinois, USA) by Frank Lloyd Wright. These two designs have been chosen because they are both well known and extensively documented, and they also represent two contrasting architectural styles (respectively Functionalist Modernism and the Prairie Style). Because the focus of the paper is on developing a new method, these two designs are merely indicative of the potential of this approach and its capacity to work in different contexts; in the former case, the *Villa Savoye*, a stark, white, geometric composition, and in the latter, the *Dana-Thomas house*, a cruciform pavilion and courtyard plan.

This paper is organised as follows: (a) Perception: describes methods of extracting 3D isovist from Google Sketchup models; (b) Data organisation: describes various techniques employed for organising the data into a workable form; (c) Saliency modelling: describes the underlying method of principal component analysis employed to extract inherent structural variation and options for comparison of the extracted information; (d) Experiments: describes different techniques of experimentation on the selected archetypal models and the most salient, and least salient regions identified for each; and finally, (e) discussion and conclusion are presented. This paper develops and expands on the methods and results recorded in previous research by the authors (Bhatia et al., 2012).

Because the paper is largely concerned with methodological innovation and a demonstration, rather than a complete validation of an approach, there remain several facets that are unable to be developed in full in the present work. For example, while it might be useful to try to identify a “saliency scale” which has a more universal

application, a much larger set of cases would need to be analysed before this could occur. Similarly, this paper cannot propose an ideal level of saliency for a designer to attempt to achieve, or a planner to attempt to legislate. The capacity to recognise and measure saliency is a sufficiently complex problem in itself, as too is the use of data derived from three-dimensional isovists, that such issues are outside the scope of the present paper.

## **2. Perception**

Conceptually, an isovist is a way of representing the amount of space that is visible from a particular vantage point. It is a geometric, and thereby measurable, representation of the experience of human sight. However, in practice the “visible space” that the isovist records is typically approximated to a horizontal slice, taken parallel to the ground at eye-height, through the 3D visible volume (Benedict 1979). Once the 2D isovist has been developed, then it is possible to quantitatively analyse its geometry to obtain various insights into the design properties of an architectural plan (Batty 2001; Turner *et al.* 2001). While 2D isovist analysis has dominated this field of inquiry, other researchers have set out to include the third dimension (Derix and Gamlesæter, 2008; Morello and Ratti, 2009; Bartie *et al.*, 2010; Suleiman *et al.*, 2011; Suleiman *et al.*, 2013). Adding the third dimension poses particular challenges pertaining to the availability of stable and translatable 3D models and the requirement of a high level of computational power. Therefore, previous attempts to analyse 3D isovists have adapted GIS based systems to define a viewshed as the set of grid cells in a Digital Elevation Model (DEM) that can be seen from a vantage point using ray casting (Llobera 2003; Ratti 2005; Bartie *et al.*, 2010; Suleiman *et al.*, 2011; Suleiman *et al.*, 2013). Such methods adapted approximate visibility analysis techniques to achieve computational efficiency. Other approaches to 3D isovist analysis include the

development of a Spatial Openness Index (SOI); the ratio between the volume of the built structure and the area of the environment enveloping it (Fisher-Gewirtzman and Wagner 2003). Importantly, research employing 3D isovists, has recognised and asserted the utility of adding a third dimension for understanding visual perception and its effects (Derix and Gamlesæter, 2008; Morello and Ratti, 2009). Especially, for the purpose of analysing spatial identity and wayfind-ability, the 2D variation is too abstract; it is effectively missing a large amount of the spatial information that is critical for determining saliency. Thus, to ensure both the accuracy and the usefulness of the method the present paper uses a computationally efficient, holistic model of 3D isovist generation and analysis. While not the central outcome of the present paper, this is, in itself, a new technique that has not previously been used in architectural or urban analysis.

### ***2.1 Google Sketchup recording***

Despite the development of modern 3D visualization and design software, many of the standard CAD formats used in architectural practice are unusable for the purpose of generating isovists because they embed an excess of information into the geometric properties of the model. In response to this problem, the present research uses *Sketchup's* (Trimble Sketchup 2012) 3D virtual walk simulation in combination with a customised *Ruby* script (Sketchup Ruby Scripts 2012) to extract 3D Isovists. In this way the user effectively “walks” through and thereby explores the model in a methodical way, while the *Ruby* script records a series of coordinates, which locate the user’s position along a path. Once the plan has been methodically investigated the recording is stopped and the collection of coordinates that have been visited are indexed. These indexed coordinates become the basis for the set of 3D isovist vantage points to be computed from the model. Figure 1 illustrates a set of adjacent frames recorded during

the walk-through experience of a Sketchup model and an illustration of the path generated during the walk.

-----  
Figure 1 comes here  
-----

## ***2.2 3D Isovist representation***

Capturing the geometrical abstractions of visible space in this paper is achieved by the use of traditional ray-casting techniques in 3D. Ray casting in this context refers to the general problem of determining the first object intersected by a ray, in common terms this process is sometimes known as ray-testing. To generate a 3D isovist, rays are projected from a fixed height  $h$  at a vantage point index  $i$  to cover the full  $360^\circ$  horizontal view orientation as well as a  $0^\circ$  to  $180^\circ$  vertical view orientation. The lengths of projected rays are represented as  $r_{\theta,\varphi}$ , the subscript  $\theta$  and  $\varphi$  indicate the corresponding values of horizontal and vertical directions respectively. The complete set of these ray lengths is combined together to form one isovist dataset. In general, the existing methods of analysing 3D isovists would represent the entire space in the form of one such dataset. However, due to the fixed value of height at which the isovist is recorded, the dataset remains biased to represent the visual space, as seen by a person of height  $h$ . To overcome this limitation, in the present research the ray projection is repeated at incremental height levels while maintaining the horizontal location of the vantage point. Thus, this method is akin to constructing a dense, vertically layered, series of three-dimensional isovists. The complete isovist dataset recorded at a vantage point can therefore be represented as  $r_{\theta,\varphi,h}$  where the additional subscript  $h$  stands for height. Though other methods of information extraction, including direct mining from

model data, are possible, the present variation of the traditional 3D ray casting approach more closely imitates the human experience of space. Additionally, it caters for 3D space that is visible to humans belonging to different height, age or mobility groups (from short to tall, from children to adults, from people in wheelchairs, to those in cars, trucks or buses) and thereby serves as a platform for future studies into the impact of architectural space on people with differing view positions.

---

Figure 2 comes here

---

### ***2.3 Sketchup isovist generation***

After the recording of vantage points, the customized *Ruby* script interacts with *Sketchup* via its Application Programming Interface (API), to examine the ray-testing operation at a specific direction and height. *Sketchup* in turn mines the model data, and provides the length of ray between the vantage point and the first object intersected by the ray. For the case when the ray encounters an opening such as a window or a door present in the model, there are two possibilities: (i) the ray should pass through the opening and reach out to a maximum fixed value; (ii) the ray should stop at the opening and remain within the boundaries of the enclosed environment. For the present research the former interpretation is described as Fixed Length Isovists (FLIs) and the latter as Boundary Length Isovist (BLIs). Figure 2 illustrates the difference in method of 3D isovist generation for the two cases of BLI and FLIs. Depending on the location of the building under consideration, the view of the outside world could contribute as an attractive spot, or be accounted for as an area that does not offer much privacy. In this

study, we compare and contrast the impact on structural variability by the choice between FLI and BLIs.

---

Figure 3 comes here

---

---

Table 1 comes here

---

#### ***2.4 Isovist data visualization***

Recording isovists at multiple heights, apart from capturing different viewpoints of visible space, also provides a significant amount of co-related information by producing approximately  $6.5 \times 10^5$  ray lengths per vantage point. To obtain meaningful insights from this data it is important to isolate the co-related repetitive information and retain essential summaries. In the present research, these summaries are obtained by transforming the original isovist dataset into its statistical derivatives. Considering the original dataset containing ray lengths  $r_{\theta,\varphi,h}$ , statistical summaries of  $r$  can be obtained over one of  $\theta$ ,  $\varphi$ , or  $h$ . Depending on the nature of statistic used (mean, variance, maximum, minimum and like), the original dataset can be translated to provide different insights into the spatial structure. Each of these summaries are represented as  $Z_{min}$ ,  $Z_{max}$ ,  $Z_{var}$ . Mathematically as an example summarised over  $\varphi$ ,  $Z_{max}^{\varphi} = \{max_{\varphi} r_{\theta,\varphi,h} : h \in [h_{min}, h_{max}], \theta \in [0,360], \varphi \in [0,180]\}$  represents the set of all longest ray lengths recorded in each horizontal direction and at each height. In other words,  $Z_{max}^{\varphi}$  represents an isovist comprising maximal visibility ray lengths. Various  $Z$  statistics along with their interpretations are provided in Table 1. Apart from providing

useful insights into the structure, each of the  $Z$  statistics can be visualized for each height separately, or collectively for all heights in the form of a heatmap. A heatmap is a graphical representation of data present in a 2D matrix, generated by assigning a colour to each data value present in the matrix. Visualising for each height level, Figure 3 represents  $Z_{max}$  and  $Z_{mean}$  (ordinate) of a BLI and a FLI, observed at a fixed height level as opposed to horizontal direction between 0 and 360 degrees (abscissa). The plots demonstrate the changes observed when visualising the same area, but from different polar angle orientations. The current plot has limited usage as the height is fixed. Visualising all heights collectively can be done using a heatmap matrix where each cell/pixel/unit of the matrix corresponds to one colour in the map. The rows of matrix represent different heights, and the columns correspond to different azimuthal directions. Figure 4 presents a heat map for  $Z_{max}$  computed on corresponding FLI and BLI along with the associated view from the vantage point in the model. The colour-bar provided on the right side of the figure demonstrates the scale of variations of  $Z_{max}$  values presented by the heatmap.

-----  
Figure 4 comes here  
-----

### 3. Saliency Estimation

The proposed method for detecting salient regions is based on the technique of Principal Component Analysis (PCA) (Jolliffe 2002). PCA is a mathematical procedure that transforms observed high dimensional data to a low dimensional set of observations, while retaining maximum information. The process involving PCA identifies the data values that have a high level of correlation, and removes them. As a result, only the most relevant observations are retained. The transformed low

dimensional data is in the form of one or more low-dimensional vectors known as Principal Components. The principal component vectors are linearly independent, and are considered as a concise summary of the high dimensional dataset from which they are obtained. Through the application of PCA on the heatmap data, a compact set of these linearly uncorrelated vectors or principal components are obtained. Principal vectors, being concise identifiers/descriptors of the heatmaps of different vantage point locations, are compared to identify the ones that are salient. The rest of this section details the procedure of extracting principal components, measures of saliency, and methods of comparison.

---

Figure 5 comes here

---

### ***3.1 Principal Component Analysis***

$Z_{var}^{\varphi}$  Heatmap is a visual representation of the set  $Z_{var}^{\varphi}$ . Each pixel in the heatmap is indexed by the heights and the horizontal direction at which each entry in  $Z_{var}^{\varphi}$  is computed. By the process of isovist generation, it is common to have similar values of ray lengths corresponding to adjacent horizontal directions of projection. This redundancy not only adds insignificant dimensions to the data, but also makes the data difficult to compare. Thus, PCA is used here for extracting significant data from the heatmap. Principal components extracted via PCA contain significant information present in the original heatmap. The effect of applying PCA on the heatmap can be visualised in Figure 5. The original heatmap, comprising 360 columns (one for each direction) is reduced to  $n$  columns ( $n \ll 360$ ). The quantity  $n$  is the number of principal components that are extracted, which may be different for each heatmap. For complex heatmaps that contain a large amount of uncorrelated information, the value of  $n$  would

be higher and vice versa. These  $n$  column vectors are sufficient to categorize a heatmap and compare it with other heatmaps. The process of computing these principal components involves extraction of eigenvalues and eigenvectors of the covariance matrix of the given heatmap. A total of 360 eigenvectors are extracted from the covariance matrix. Each eigenvector has a set percentage contribution towards the total information contained in the heatmap. These percentage contributions are computed by evaluating their respective eigenvalues. Let  $\lambda_i$  represent the eigenvalue corresponding to  $i^{\text{th}}$  eigenvector, and let  $\Lambda = \lambda_1 + \lambda_2 + \dots + \lambda_{360}$ . Then the percentage contribution  $P_i = (\lambda_i \times 100) / \Lambda$ . Using the values of  $P_i$  vectors that describe at least 95% of the total uncorrelated information are selected. In combination, the extracted set of these vectors form a Principal Component Subspace, or simply subspace. This subspace essentially provides a low-dimensional set of basis vectors onto which the original heatmap dataset is projected. The new reduced dataset obtained by this projection of original data onto its principal subspace is termed as “scores”. Each of these subspaces and scores are then evaluated using the stated saliency measures described in the next section. Readers interested in detailed process of performing PCA are advised to refer to Jolliffe (2002).

### ***3.2 Saliency Metric***

The saliency metrics used in this paper examine the difference between two principal component scores. As a result, each measure stipulates a number between zero and one, wherein zero denotes minimum difference and one denotes a completely different score and hence a different heatmap. The comparison reveals the extent to which one heatmap (and hence one location) is different from others, thereby suggesting a method for identifying the location that is most different from all others in a given set.

Consider two vantage point indices  $G$  and  $H$ . Post PCA computation, for each location

its corresponding scores are available. Let  $L$  and  $M$  be the corresponding score for vantage points  $G$  and  $H$ . Let  $L$  and  $M$  contain  $i$  and  $j$  column vectors, respectively. Based on this indexing, we define two saliency metrics: (i) Angle between subspaces (ii) Entropy of subspace. Each metric is computed independent of the other, and finally combined and normalised to obtain an overall account of inherent saliency.

### 3.2.1 Angle between subspaces

The first saliency measure employed in this paper compares the angle between these two subspaces. It is derived from the similarity factor defined by Krzanowski (1979) who developed a method to measure the similarity between two principal component subspaces. For the present application, the complement of this measure was used to quantify the difference between two scores  $L$  and  $M$ ; a difference denoted as  $S_{GH}$ . The subscripts  $G$  and  $H$  denote the indices of the associated vantage points. Originally, similarities between subspaces were defined, following Krzanowski (1979) as:  $Similarity = trace(L^T M M^T L) / k$ . The superscript  $T$  represents transpose. In this definition, it is assumed that both  $L$  and  $M$  have the same number of column vectors viz.  $k$ . For our application, this definition is modified to allow them to have different numbers of column vectors. Let  $K = (i + j) / 2$ , the saliency measure,  $S_{GH}$ , is then computed as the inverse of the similarity, defined in equation 1.

$$S_{GH} = \frac{K}{trace(L^T M M^T L)} \quad (1)$$

### 3.2.2 Entropy of subspace

Entropy (Shannon 1948) provides an account of the informative content of a dataset. The second measure of saliency used in this work is defined using the entropy of the scores. Consider, for example, a heat map matrix for an isovist at vantage point index  $G$ ,

and its corresponding score matrix  $L$ , obtained after PCA. Let the score matrix consist of  $i$  column vectors. Entropy is calculated on the histogram of the values in each column vector of  $L$ . The histogram divides the entire range of values in suitable equal size intervals, and counts the number of values present in each interval. The entropy value is then computed on the counts present in each histogram interval. Thus, let  $p_i$  represent the  $i^{\text{th}}$  interval, and let  $m$  be the total number of intervals present, then the entropy  $E_G$  for the isovist at  $G$  is defined in equation 2. The values of  $E_G$  are scaled between zero and one. The higher  $E_G$  value for a vantage point index reveals higher uniqueness of that location in comparison to others being considered for comparison.

$$E_G = - \sum_{i=0}^m p_i \cdot \log(p_i) \quad (2)$$

## 4. Experiments and Results

### 4.1 Experimental Setup

This section describes the experimental setup used to compare salient regions present in the *Villa Savoye* and *Dana-Thomas House* models using the previously presented methods. Each model was explored using the Google Sketchup walk tool, and the additional script was used to record vantage points and generate BLI and FLIs. To ensure non-redundancy, a minimum distance of 1 meter was obtained between two horizontal vantage point locations. The spatial coordinates recorded during the walk performed comprise a series of ordered vantage point coordinates. These vantage point coordinates were indexed for easy reference, and corresponding to each index, the isovist matrix,  $Z_{var}^{\phi}$ , its heatmap and finally the principal component scores were computed. Therefore, to address a vantage point, its associated view and data, its index was used and a correspondence between the index and vantage point location was

maintained together in a set labelled as  $\Sigma$ . The given setup presented two choices of analysis: (i) Comparison between one location to all other locations in the entire model, we call this Global Saliency; (ii) Subdivision of the entire model into smaller regions, followed by comparison of a location in a selected region with all other locations within the same region, termed as Local Saliency. We adopt the term “location” as the area associated with one recorded vantage point, and the term “region” as a collection of neighbouring  $n$  locations. As an example, local saliency computed on a dataset containing 50 “neighbouring” vantage points can be used to identify the most salient location in the small region of the environment.

#### ***4.2 Computation***

Sketchup models of the *Dana-Thomas House* and the *Villa Savoye* were used to record a total of 300 vantage points covering the entirety of each model. Local saliency was computed over two different experiments. First, by distributing the 300 points into three regions each containing 100 locations. Second by distributing into six regions each containing 50 locations. The saliency computation was performed taking one region at a time. Conversely, global saliency was computed over the entire dataset considering one location at a time. The dataset was generated on a Windows-based desktop PC with 16-GB RAM, and equipped with Intel Core i7 processor, running Sketchup and the additional Ruby plugin. Final computations of principal components and salient regions were performed in MATLAB<sup>TM</sup> R2011. The generation of isovists at each height level in Sketchup took an average of one minute per vantage point. MATLAB<sup>TM</sup> scripts for computation of principal components (including importing data, computation and saving the principal components) took an average of seven seconds per vantage point.

### 4.3 Global Saliency Results

Evaluation of global saliency in the present analysis can be interpreted over different types of heatmaps (Table 1). To illustrate their utility and differences, global saliency computation was performed over  $Z_{var}^{\varphi}$  and  $Z_{mean}^{\varphi}$  heatmaps. The results are presented in Figure 6. The first part of the Figure 6(a) illustrates the combined saliency value corresponding to each vantage point location index. The graphs compare the global saliency values, obtained for BLI and FLIs for the *Villa-Savoye* and the *Dana-Thomas House* using  $Z_{var}^{\varphi}$  and  $Z_{mean}^{\varphi}$ . The vantage point locations having highest (green marker) and lowest saliency (red marker) values are illustrated. Saliency values were found to be different in BLIs and FLIs for locations with openings (such as doors). This is due to the incorporation of variability present in area visible from any window or opening of the model in the case of FLIs. Corresponding views for the 4 most extreme saliency values (highest 4, and lowest 4) are presented in Figure 6(b). Through this process  $Z_{var}^{\varphi}$  heatmaps revealed locations with maximum/minimum variance of structure, while use of  $Z_{mean}^{\varphi}$  heatmap revealed locations with maximum/minimum visibility from vantage point.

-----  
Figure 6 comes here  
-----

In the *Villa-Savoye* model, the terrace with clear views of the spiral staircase and the inclined ramp was identified to be the most salient region using BLI. The identified least salient region was the passage between two rooms comprising of parallel walls and with no variability in its spatial structure. Wright's *Dana-Thomas House* has a complex, cruciform plan, with several well-defined exterior courtyard spaces, which have generated some of the most salient views. Of the interior spaces, both the private living

room and the grand dining room offer high levels of spatial difference. There are multiple corridors linking these major spaces, along with several exterior walls to service areas, which all have low levels of saliency.

#### ***4.4 Local Saliency Results***

Performing saliency evaluation on a small cluster of all neighboring vantage points is instrumental in identifying the salient locations present within a small region of the entire environment. Figure 7 illustrates the results of two local saliency experiments. First by clustering 100 vantage points in a region, and second by clustering 50 vantage points. The analysis was performed on  $Z_{var}^{\phi}$  heatmaps for *Villa-Savoie* and *Dana-Thomas house*. Figure 7(a) consists of 6 graphs (3 for each model), and 7(b) of 12 graphs (6 for each model). The graphs represent saliency values (ordinate) of vantage point index (abscissa) relative to all neighboring locations in the region. From the graphs it can be observed that the number of locally salient regions were higher in number when comparing 100 vantage points at a time.

-----  
Figure 7 comes here  
-----

### **5. Conclusion**

When Lynch (1960) famously demonstrated that humans construct their understanding of complex spaces using particular sets of visual cues (including landmarks and boundaries), he effectively revolutionised the way architects and urban designers thought about spatial identity. He also postulated various conditions under which a person is more or less likely to be lost when navigating across a city, or experiencing a large building for the first time. While many studies have since

reinforced the importance of Lynch's insights, practical applications to model, analyse and optimise architecture to accommodate such ideas have not yet been developed. With the rise in importance of computational modelling (CAD, BIM, parametric and generative models) for both the design and analysis of space, there is a growing need for systems or approaches that can support a heightened understanding of existing environments and an improved capacity to design new ones. While the present study cannot yet reach that level of useability, it offers an important first step, by demonstrating a new, stable and repeatable process for generating 3D isovists to provide a unique methodology for measuring visual salience in an architectural environment. Using a statistical approach to processing data obtained from different sections of an architectural model, the paper compares this data using PCA and entropy to reveal differences in spatial structure of each section. This process is then used to measure relative saliency; the capacity for the view from a particular position to differ from that of the rest of the location. This new methodology is capable of being altered in multiple ways although the variation demonstrated using isovist ray lengths produces consistent and useful results. Future developments of this research will consider the inclusion of colour variations along with a version of the pure geometrical methodology for saliency computation.

Finally, while neither comprehensive nor specifically for this purpose, the results of the saliency analysis of the Villa Savoye do broadly correlate with several previous interpretations of the spatial identity of this building. Such readings suggest that certain elements, like the spiral staircase and the roof terrace contain a high level of specific spatial information and are thus salient or landmark locations, while others are more uniform or undifferentiated (Figure 6(b)). In the case of the *Dana-Thomas House*, Hildebrand (1991) argues that Frank Lloyd Wright's domestic architecture often

possesses a pattern of discovery that draws a visitor from the entry to the living room, gradually revealing the spatial particularities of the design. The saliency results for the *Dana-Thomas House* broadly support this theory, but without a more detailed analysis, it is difficult to draw particular conclusions about this house or wayfinding and Wright's Usonian architecture.

## **6. Acknowledgement**

This project is supported by ARC DP1092679: "Modelling and predicting patterns of pedestrian movement: using robotics and machine learning to improve the design of urban space.". The 3D models used for the test were obtained from the Google *Sketchup* Warehouse (*Villa Savoye* by Keka; *Dana-Thomas House* by Joe Sweeney).

## **References**

- Bartie, P., F. Reitsma, S. Kingham, and S. Mills. 2010. "Advancing Visibility Modelling Algorithms for Urban Environments." *Computers, Environment and Urban Systems* 34(6): 518–31.
- Baskaya, A., Wilson, C., and Özcan, Y. Z. 2004. "Wayfinding in an Unfamiliar Environment: Different Spatial Settings of Two Polyclinics." *Environment and Behavior* 36(6): 839–867.
- Batty, M. 2001. "Exploring Isovist Fields: Space and Shape in Architectural and Urban Morphology." *Environment and Planning B: Planning and Design* 28(1): 123-150.
- Benedikt, M. L. 1979. "To take hold of space: Isovists and Isovist Fields." *Environment and Planning B: Planning and Design* 6(1): 47-65.
- Bhatia S., Chalup S. K., and Ostwald M. J. 2012, "Analyzing Architectural Space: Identifying Salient Regions by Computing 3D Isovists," In Proceedings of 46th Annual Conference of the Architectural Science Association.
- Caduff, D., and S. Timpf. 2008. "On the assessment of Landmark Saliency for Human Navigation." *Cognitive Processing* 9(4): 249–67.

- Carlson, L. A., Hölscher, C., Shipley, T. F., and Conroy-Dalton, R. 2010. "Getting Lost in Buildings." *Current Directions in Psychological Science* 19(5): 284-289.
- Conroy-Dalton, R. 2001. "Spatial Navigation in Immersive Virtual Environments." PhD diss., The University of London.
- Conroy-Dalton, R. 2005. "Space Syntax and Spatial Cognition." *World Architecture: Space Syntax Monograph* 11(185): 41-45.
- Derix, C., and Å. Gamlesæter. 2008. "3d Isovists and Spatial Sensations: Two methods and a case study" Paper presented at the Environmental Design Research Association 39th Annual Conference: Movement and Orientation in Built Environments: Evaluating Design Rationale and User Cognition.
- Duckham, M., S. Winter, and M. Robinson. 2010. "Including Landmarks in Routing Instructions." *Journal of Location Based Services* 4(1): 28–52.
- Ellard, Colin 2009. "You Are Here." New York: Random House.
- Fisher-Gewirtzman, D., and Wagner, I. A. 2003. "Spatial Openness as a practical metric for evaluating built-up Environments." *Environment and Planning B: Planning and Design* 30(1): 37-49.
- Golledge, R. G. 1999. "Human Wayfinding and Cognitive maps." Chap. 1 in *Wayfinding Behavior: Cognitive Mapping and other Spatial Processes*. Baltimore: Johns Hopkins University Press.
- Han, X., P. Byrne, M. Kahana, and S. Becker. 2012. "When Do Objects Become Landmarks? A VR Study of the Effect of Task Relevance on Spatial Memory." *PLoS One* 7(5): e35940.
- Haq, S., and Giroto, S. 2003. "Ability and Intelligibility: Wayfinding and Environmental Cognition in the Designed Environment." Paper presented at the 4th International Space Syntax Symposium, London, 68.1-68.20.
- Hildebrand, G. 1991. "The Wright Space: Patterns & Meaning in Frank Lloyd Wright's Houses." Seattle: University of Washington Press.
- Hirtle, S. 2008. "Landmarks for Navigation in Human and Robots." Chap. 9 in *Robotics and Cognitive Approaches to Spatial Mapping*, Springer Tracts in Advanced Robotics 38: 203-214.
- Hochdorfer, S., and C. Schlegel. 2009. "Landmark Rating and Selection According to Localization Coverage: Addressing the challenge of lifelong operation of slam in service robots." Paper presented at the IEEE/RSJ International Conference on Intelligent Robots and Systems 382–87.

- Jolliffe, I. T. 2002. Principal component analysis. Vol. XXIX of Springer Series in Statistics 2nd ed. New York: Springer.
- Llobera, M. 2003. "Extending GIS-based Visual Analysis: the concept of Visualscapes." *International Journal of Geographical Information Science* 17(1): 25-48.
- Lynch, K. 1960. "The Image of the City." Cambridge, MA: MIT Press.
- Meilinger, T., Franz, G., and Bühlhoff, H. H. 2012. "From Isovists via mental representations to Behaviour: First steps toward closing the causal chain." *Environment and Planning B* 39(1): 48-62.
- Miller, J., and L. Carlson. 2010. "Selecting Landmarks in Novel Environments." *Psychonomic Bulletin & Review* 18(1): 184-91.
- Montello, D. R. 1998. "A New Framework for Understanding the Acquisition of Spatial Knowledge in Large-scale Environments." Chap. 11 in M.J. Egenhofer, R.G. Golledge. eds. *Spatial and Temporal Reasoning in Geographic Information Systems*. Oxford, New York: Oxford University Press.
- Morello, E., and Ratti, C. 2009. "A Digital Image of the City: 3D Isovists in Lynch's Urban Analysis." *Environment and Planning B: Planning and Design* 36(5): 837-853.
- Peters, D., Y. Wu, and S. Winter. 2010. "Testing Landmark Identification Theories in Virtual Environments." *Spatial Cognition VII, Lecture Notes in Computer Science*, Christoph Hölscher, Thomas Shipley, Marta Olivetti Belardinelli, John Bateman, and Nora Newcombe eds. Springer Berlin / Heidelberg 6222: 54-69.
- Ratti, C. 2005. "The Lineage of the Line: Space syntax parameters from the analysis of urban DEMs." *Environment and Planning B* 32(4): 547-566.
- Röser, F., A. Krumnack, K. Hamburger, and M. Knauff. 2012a. "A Four Factor Model of Landmark Salience—A new approach." In N. Rußwinkel, U. Drewitz & H. van Rijn eds., *Proceedings of the 11th International Conference on Cognitive Modeling*, Berlin: Universitaetsverlag der TU Berlin 82-87.
- Röser, F., K. Hamburger, A. Krumnack, and M. Knauff. 2012b. "The Structural Salience of Landmarks: Results from an on-line study and a Virtual Environment Experiment." *Journal of Spatial Science* 57(1): 37–50.
- Sketchup Ruby Scripts 2012. "Google Sketchup, Ruby Scripts.", <http://www.sketchup.com/intl/en/download/rubyscripts.html>.

- Suleiman, W., T. Joliveau, and E. Favier. 2011. "3D Urban Visibility Analysis with Vector GIS Data." In Jones C. E., Pearson A., Hart G., Groome N. eds. , Proceedings of the 19th GIS Research UK Annual Conference, University of Portsmouth 2011, 27–29.
- Suleiman, W., T. Joliveau, and E. Favier. 2013. "A New Algorithm for 3D Isovists." In Sabine Timpf and Patrick Laube eds., Advances in Geographic Information Science, Advances in Spatial Data Handling. Springer Berlin Heidelberg 157–73.
- Trimble Sketchup 2012. "Google Sketchup." <http://sketchup.google.com/intl/en/>.
- Turner, A., Doxa, M., and O'Sullivan, D. 2001. "From Isovists to Visibility Graphs: a Methodology for the Analysis of Architectural Space." Environment and Planning B: Planning and Design, 28(1): 103-121.
- Werner, S. 2004. "The role of Spatial Reference Frames in Architecture." Environment and Behavior 36(4): 461-482.
- Wiener, J. M., and Franz, G. 2005. "Isovists as a means to predict spatial experience and behavior." Spatial Cognition IV, Reasoning, Action, Interaction 3343: 42-57.
- Wiener, J. M., Franz, G., Rossmannith, N., Reichelt, A., Mallot, H. A., and Bühlhoff, H. H. 2007. "Isovist Analysis captures properties of space relevant for Locomotion and Experience." Perception 36(7): 1066-1083.
- Winter, S., M. Tomko, B. Elias, and M. Sester. 2008. "Landmark Hierarchies in Context." Environment and Planning B: Planning and Design 35(3): 381-98.

$Z$	Interpretation
$Z_{max}^{\varphi}, Z_{min}^{\varphi}, Z_{diff}^{\varphi}$	Maximum, minimum and difference (max – min) in visibility over $\theta$ , $\varphi$ and $h$ measured for each azimuthal direction, for all heights.
$Z_{mean}^{\varphi}, Z_{var}^{\varphi}$	Mean and variance in visibility in over $\theta$ , $\varphi$ and $h$ measured at different heights.
$Z_{max}^h, Z_{min}^h, Z_{diff}^h$	Maximum, minimum and difference (max – min) in visibility over $\theta$ , $\varphi$ and $h$ measured for each azimuthal and polar directions.
$Z_{mean}^h, Z_{var}^h$	Mean and variance in visibility over $\theta$ , $\varphi$ and $h$ measured for each azimuthal and polar directions.

Table 1. Various  $Z$  statistics that can be obtained over  $r_{\theta,\varphi,h}$ , and their interpretations.

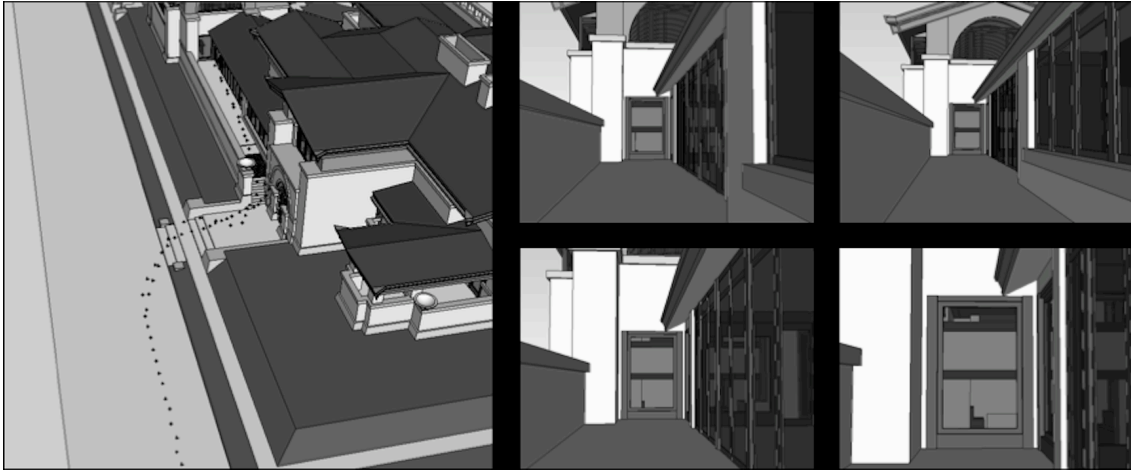


Figure 1. Path generated during Sketchup walk (left); A small subset of adjacent frames recorded during the walk (right).

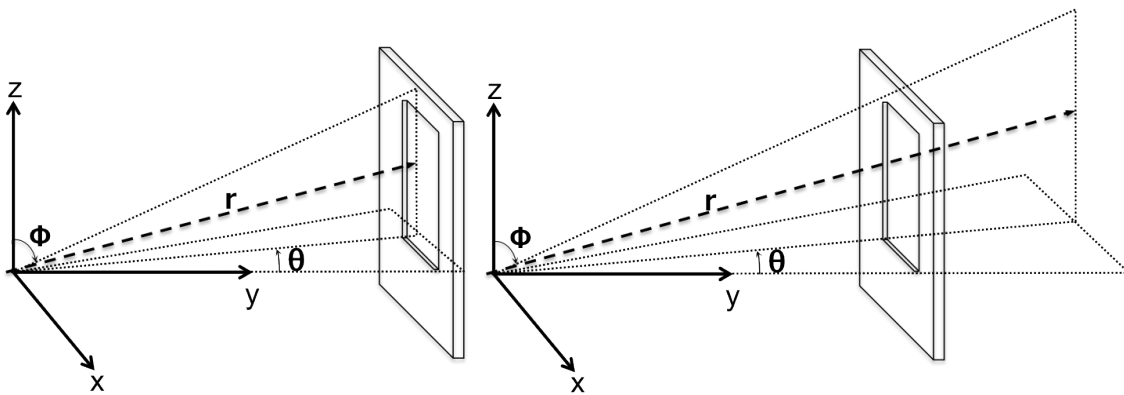


Figure 2. Illustration of how the ray projection is handled during the generation of isovists for the two cases of BLI (left), FLI (right). FLIs being of fixed length (which is usually chosen as a large value) tend to travel beyond any present openings.

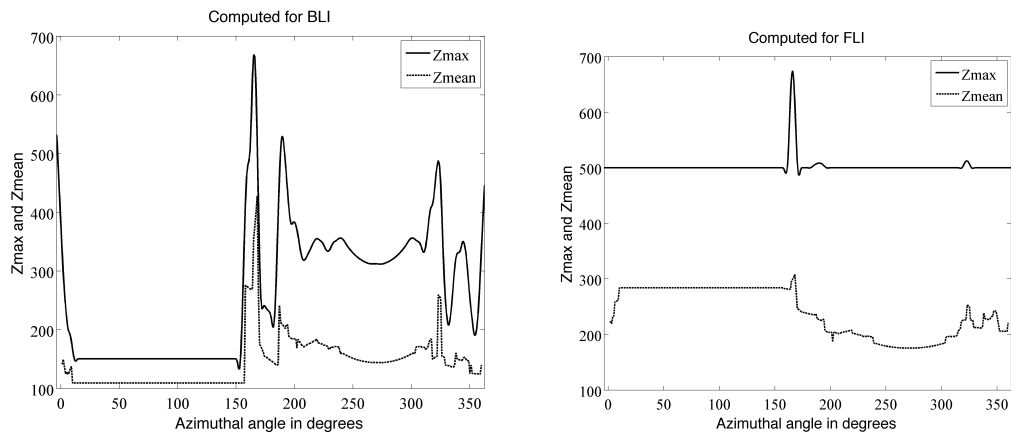


Figure 3.  $Z_{max}$  and  $Z_{mean}$  (ordinate) computed for a fixed height level vs. horizontal direction between 0 and 360 degrees (abscissa) for a BLI (left) and FLI (right). As evident, the  $Z_{max}$  values are higher than those of  $Z_{mean}$ .

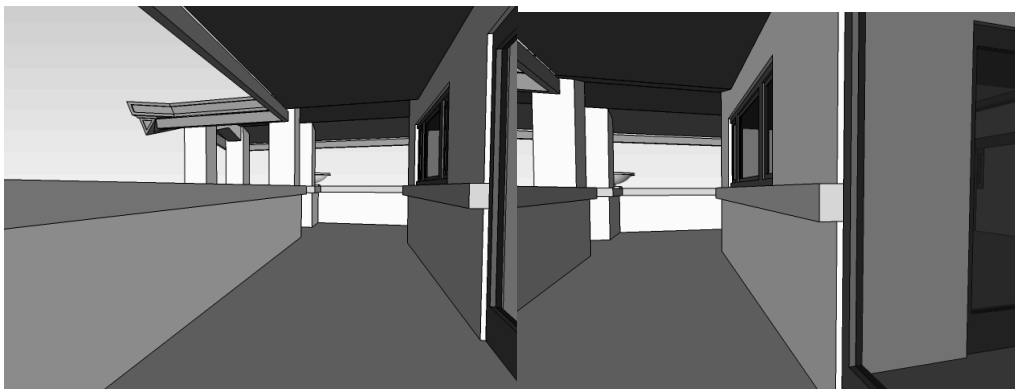
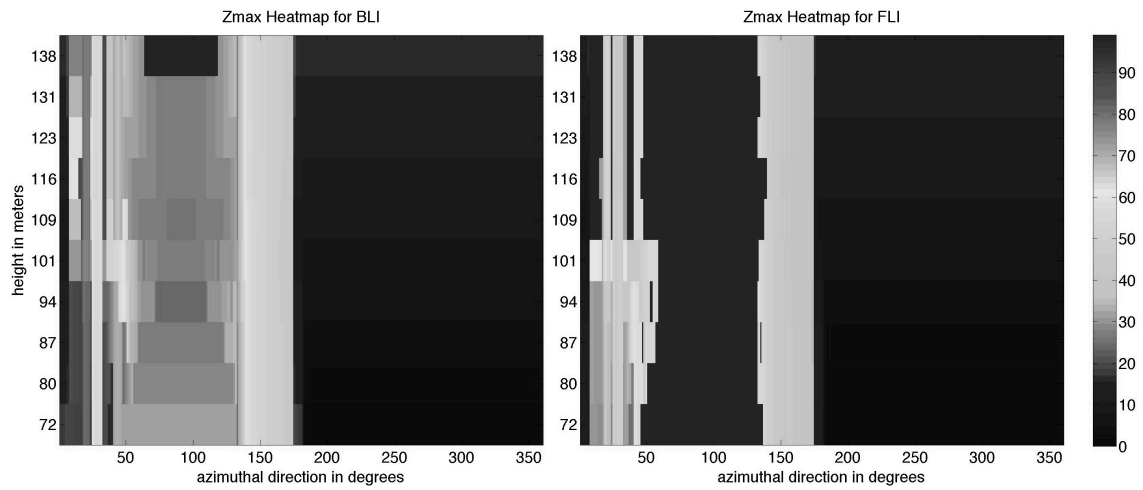


Figure 4. Heat map for  $Z_{max}$  computed on corresponding BLI (left) and FLI (right) along with the associated views from the vantage point in the model (bottom row). As FLI isovist rays are allowed to pass through the windows or openings, they are typically longer. This can be observed by comparing the two heatmaps, where FLI heatmap shows more colour variation corresponding to longer ray lengths.

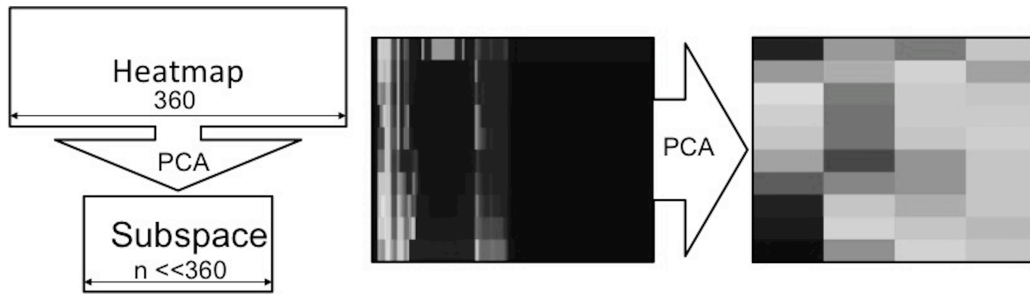
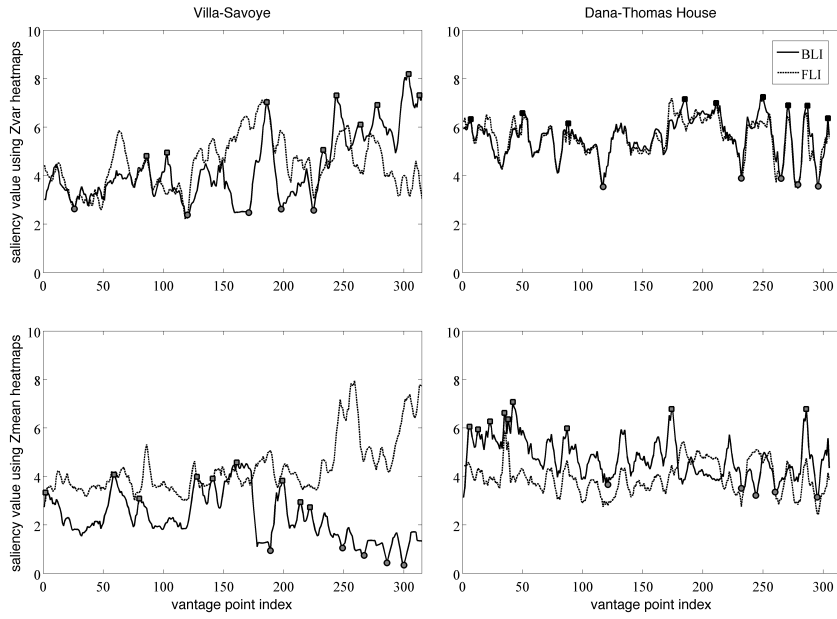
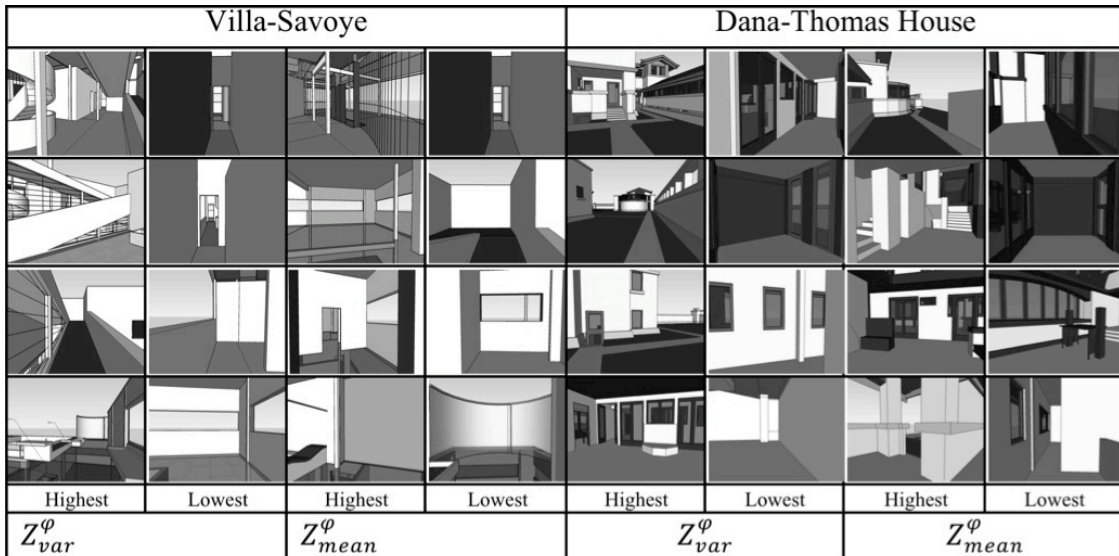


Figure 5. Effect of applying PCA (left), demo transformation of a heatmap matrix into its principal component scores. The original heatmap/matrix comprising of 360 columns is reduced to a 4-column heatmap/matrix.

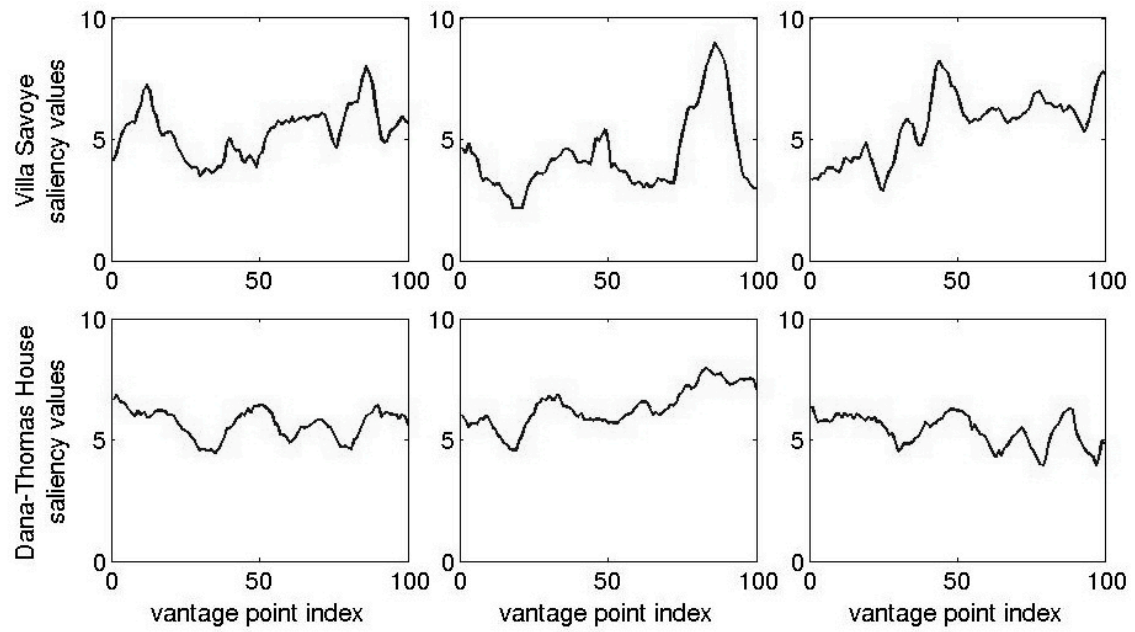


(a)

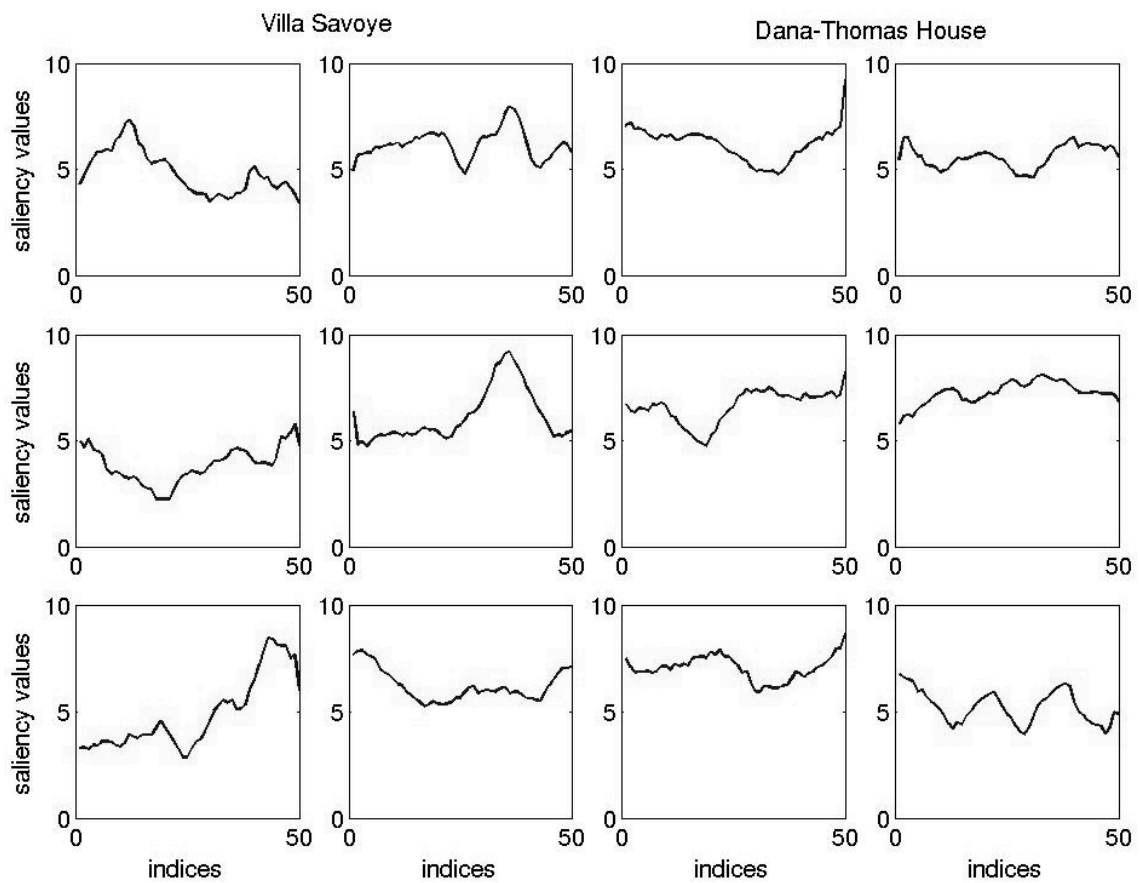


(b)

Figure 6. Global saliency values for Villa-Savoye and Dana-Thomas house computed using  $Z_{var}^{\phi}$  (6a top row) and  $Z_{mean}^{\phi}$  (6a bottom row) heatmaps, with corresponding views of locations with highest and lowest saliency values in 6b. The number of peaks indicates the presence of many salient locations in the corresponding environments.



(a)



(b)

Figure 7. Local saliency values computed over BLIs using  $Z_{var}^{\varphi}$  heatmaps, illustrating uniqueness of corresponding vantage point locations relative to the others in the entire region (comprising neighbouring 100 locations in 7a, and 50 locations in 7b).